Development 138, 3441-3449 (2011) doi:10.1242/dev.065961
© 2011. Published by The Company of Biologists Ltd

Kif3a regulates planar polarization of auditory hair cells through both ciliary and non-ciliary mechanisms

Conor W. Sipe and Xiaowei Lu*

SUMMARY

Auditory hair cells represent one of the most prominent examples of epithelial planar polarity. In the auditory sensory epithelium, planar polarity of individual hair cells is defined by their V-shaped hair bundle, the mechanotransduction organelle located on the apical surface. At the tissue level, all hair cells display uniform planar polarity across the epithelium. Although it is known that tissue planar polarity is controlled by non-canonical Wnt/planar cell polarity (PCP) signaling, the hair cell-intrinsic polarity machinery that establishes the V-shape of the hair bundle is poorly understood. Here, we show that the microtubule motor subunit Kif3a regulates hair cell polarization through both ciliary and non-ciliary mechanisms. Disruption of Kif3a in the inner ear led to absence of the kinocilium, a shortened cochlear duct and flattened hair bundle morphology. Moreover, basal bodies are mispositioned along both the apicobasal and planar polarity axes of mutant hair cells, and hair bundle orientation was uncoupled from the basal body position. We show that a non-ciliary function of Kif3a regulates localized cortical activity of p21-activated kinases (PAK), which in turn controls basal body positioning in hair cells. Our results demonstrate that Kif3a-PAK signaling coordinates planar polarization of the hair bundle and the basal body in hair cells, and establish Kif3a as a key component of the hair cell-intrinsic polarity machinery, which acts in concert with the tissue polarity pathway.

KEY WORDS: PAK, Basal body, Kinesin, Organ of Corti, Planar cell polarity, Stereociliary bundle, Mouse

INTRODUCTION

Sensory hair cells in the hearing organ, the cochlea, convert sound energy into electrical signals, which are in turn transmitted to the central nervous system. The mechanotransduction organelle of the hair cell is the hair bundle, consisting of rows of actin-based stereocilia with graded heights that form a V-shaped staircase pattern. The asymmetric structure of the hair bundle renders it directionally sensitive to deflection. Hair cells are depolarized by deflections toward the tallest stereocilia, hyperpolarized by deflections toward the shortest stereocilia, and insensitive to perpendicular stimuli (Gillespie and Muller, 2009).

Because of their directional sensitivity, hair bundles in the cochlea must be uniformly oriented for correct perception of sound. In the auditory sensory epithelium, the organ of Corti (OC), the vertex of the V-shaped hair bundle on every hair cell points toward the lateral edge of the cochlear duct. The uniform hair bundle orientation is controlled by the PCP/tissue polarity pathway, which regulates cytoskeletal remodeling during tissue morphogenesis in many systems (Simons and Mlodzik, 2008). In addition, the PCP pathway is also required for extension of the cochlear duct (Rida and Chen, 2009). In PCP mutants, hair bundles are frequently misoriented relative to the mediolateral axis of the cochlea. However, the structural polarity of individual V-shaped hair bundles is not affected. Thus, planar polarization of auditory hair cells is manifested at both cell and tissue levels, which are genetically separable. Planar polarization at the single cell level is independent of the PCP/tissue polarity pathway. The molecular machinery that controls polarization of individual hair cells is poorly understood.

Department of Cell Biology, University of Virginia Health System, Charlottesville, VA 22908, USA.

*Author for correspondence (xl6f@virginia.edu)

Accepted 31 May 2011

The kinocilium, a specialized primary cilium, is thought to serve as the ‘guidepost’ for hair bundle morphogenesis (Tilney et al., 1992). The axoneme of the kinocilium extends from the basal body, which is derived from the mother centriole of the centrosome (Goetz and Anderson, 2010; Nigg and Raff, 2009). In addition to organizing the cilia, the basal body and the associated pericentriolar material (PCM) also organize cytoplasmic microtubules and anchor their minus ends (Moser et al., 2010). During development of mammalian auditory hair cells, before the onset of bundle morphogenesis, the kinocilium migrates from the center of the hair cell apex to the lateral edge of the hair cell apex. The surrounding microvilli then undergo selective elongation to form a V-shaped hair bundle, with the kinocilium at the vertex of the V next to the tallest stereocilia. Thus, migration of the kinocilium/basal body appears to be the critical polarizing event that orchestrates hair bundle morphogenesis and orientation.

Indeed, there is a growing body of evidence for a role of the kinocilium/basal body in hair bundle morphogenesis and orientation. It has been proposed that the PCP/tissue polarity pathway coordinates hair bundle orientation by controlling the direction of the kinocilium/basal body migration (Montcouquiol et al., 2003). Mutations in BBS genes that underlie Bardet-Biedl syndrome, a human ciliopathy, cause defects in hair bundle morphology and inner ear PCP in mice (May-Simera et al., 2009; Ross et al., 2005). Mouse models for human Usher syndrome type I have defects in kinocilium positioning and hair bundle fragmentation and misorientation (Lefevre et al., 2008). In particular, an isoform-specific knockout of protocadherin 15 (PCDH15-ΔCD2) caused disruption of the kinociliary links that connect the kinocilium to the adjacent stereocilia, leading to hair bundle orientation and polarity defects (Webb et al., 2011). Moreover, the Alström syndrome protein ALMS1 has been shown to localize to basal bodies of cochlear hair cells and regulate hair bundle shape and orientation (Jagger et al., 2011). Finally, a role for the kinocilium in hair cell PCP regulation has been

demonstrated by genetic ablation of the kinocilium (Jones et al., 2008). Cilia assembly and maintenance require the intraflagellar transport (IFT) process, in which particles are transported bidirectionally along axonemal microtubules (Goetz and Anderson, 2010; Nigg and Raff, 2009). Deletion of *Ift88*, which encodes one component of IFT particles, in the inner ear resulted in the absence of kinocilia and basal body migration defects, causing PCP phenotypes, including a shortened cochlear duct and hair bundle misorientation (Jones et al., 2008).

In spite of the evidence pointing to a pivotal role of the kinocilium/basal body in planar polarization of hair cells, the cellular and molecular mechanisms by which basal body migration instructs hair cell polarity remain unresolved. Because the basal body is the microtubule organizing center of the hair cell, we speculated that microtubule-dependent processes control hair cell polarization. To gain mechanistic insights into microtubule-mediated processes, we investigated the role of Kif3a, a component of the microtubule plus-end directed, heterotrimeric kinesin-II motor complex. Kinesin-II is the motor for anterograde IFT required for ciliogenesis (Goetz and Anderson, 2010). Kif3a-deficient mice lack nodal cilia, have left-right asymmetry defects and die around embryonic day 10.5 (E10.5) (Marszalek et al., 1999; Takeda et al., 1999). In addition to ciliogenesis, the kinesin-II motor is also required for intracellular transport of various cargos in different cell types (Marszalek et al., 2000; Nishimura et al., 2004; Teng et al., 2005). In this study we uncover a non-ciliary function of Kif3a crucial for basal body positioning during hair cell polarization. We show that Kif3a mediates localized p21-activated kinase (PAK) activation on the hair cell cortex, which in turn regulates basal body positioning. Together with published results, we describe a model in which Kif3a is a component of the cell-intrinsic polarity machinery.

MATERIALS AND METHODS

Mice

Animal care and use was performed in compliance with NIH guidelines and the Animal Care and Use Committee at the University of Virginia. Mice were obtained from either the Jackson Laboratory or the referenced sources, and maintained on a mixed genetic background. *Kif3a*$^{flox/flox}$ females were mated with *Foxg1-Cre; Kif3a*$^{flox/+}$*; GFP-centrin2* males to generate *Foxg1-Cre; Kif3a*$^{flox/flox}$ embryos with or without *GFP-centrin2*. For timed pregnancies, the morning of the plug was designed as E0.5 and the day of birth as postnatal day 0 (P0). The following genotyping primers were used: 5′-AGAACCTGAAGATGTTCGCG-3′ and 5′-GGCTATAC-GTAACAGGGTGT-3′ (for *Cre*); 5′-AGGGCAGACGGAAGGGTGG-3′ and 5′-TCTGTGAGTTTGTGACCAGCC-3′ (for *Kif3a*^{flox} and *Kif3a*$^{+}$); 5′-ACGACTTCTTCAAGTCCGCCATGCC-3′ and 5′-GATCTTGA-AGTTCACCTTGATGCC-3′ (for *GFP-centrin2*).

Immunohistochemistry and image acquisition

Temporal bones were dissected from embryos of the indicated age and fixed overnight in 4% paraformaldehyde (PFA) at 4°C or for 1 hour at room temperature. For dishevelled 2 immunostaining, temporal bones were fixed in 10% trichloroacetic acid for 1 hour on ice. Cochleae were then dissected out of the temporal bones in phosphate-buffered saline (PBS), and immunohistochemistry was carried out as previously described (Grimsley-Myers et al., 2009).

Z-stacks of images were collected on a Deltavision deconvolution microscope using a 60× objective (NA 1.4) at 0.2 μm intervals and processed with the Softworx software package (Applied Precision) and Adobe Photoshop (Adobe Systems). Alternatively, images were collected using a Zeiss LSM 510 Meta confocal microscope. Optical slices along the *z*-axis were generated using the Volocity software package (PerkinElmer). All micrographs shown were taken from the mid-basal region of the cochlea unless otherwise indicated.

Antibodies

The following primary antibodies were used for immunostaining: anti-acetylated tubulin (1:500, Sigma), anti-α-tubulin (1:1000, Sigma), anti-phospho-β-catenin (1:100, Cell Signaling), anti-phospho-PAK1/2/3 (1:200, Invitrogen), anti-dishevelled 2 (1:100, Cell Signaling), anti-frizzled 3 (1:200, a gift from Dr Jeremy Nathans, Johns Hopkins University, Baltimore, MD, USA), anti-ZO-1 (1:300, Invitrogen), anti-α-spectrin (1:100, Millipore), anti-Rac1 (1:100, Upstate). Alexa-conjugated secondary antibodies (1:1000) and Alexa- and rhodamine-conjugated phalloidin (1:100) were obtained from Invitrogen.

Scanning electron microscopy

Temporal bones were dissected from embryos of the indicated age and fixed at 4°C in 0.1 M sodium cacodylate buffer containing 4% PFA, 2.5% glutaraldehyde and 2 mM $CaCl_2$. Cochleae were then dissected from temporal bones and postfixed for 2 hours in 1% osmium tetroxide. Cochleae were dehydrated in a series of graded ethanol washes, critical point dried, mounted on metal stubs, and sputter coated with gold. Samples were imaged on a JEOL 6400 scanning electron microscope (SEM) at 20 kV.

Quantification of hair cell centriole phenotype

We observed that centriole behavior followed a developmental gradient from the base to apex along the cochlear duct. Therefore, care was taken to ensure that an equivalent mid-basal region of the cochlea was compared between experimental groups. The data presented for centriolar measurements include only those of outer hair cells (OHCs), because the tilt of the tissue surrounding and including the inner hair cells (IHCs) precluded an accurate measurement of their centriole position.

Cochlear length was determined from whole-mount images using ImageJ software (NIH). For quantification of hair bundle orientation, the angle formed by the intersection of a line drawn through the axis of symmetry of the hair bundle and one parallel to the mediolateral axis of the OC (assigned as 0°) was measured using ImageJ. Clockwise deviations from 0° were assigned positive values and counterclockwise negative values. The orientation of flat hair bundles in *Kif3a*^{cKO} mutants was apparent owing to the asymmetric distribution of short microvilli on their apical surface.

To generate rose diagrams of the planar position of hair cell centrioles, projected *z*-stacks were used to assign centriole positions to one of six 60° sectors within the hair cell. Rose diagrams were plotted using the CircStats library in the R software package (http://www.r-project.org/). To quantify the deviation of basal body position from the mediolateral axis, the intersection of a line drawn from the hair cell center through the basal body and one parallel to the mediolateral axis of the OC (assigned as 0°) was measured in ImageJ. Clockwise deviations from 0° were assigned positive values and counterclockwise negative values. Microsoft Excel was used to calculate Pearson's correlation coefficient and generate scatter plots.

To quantify hair cell centriole pair distance, the three-dimensional coordinates of each centriole were recorded using the point plotting function in Softworx. Typically, GFP fluorescence from a single centriole was visible in multiple *z*-planes. The coordinate of the plane with the brightest GFP fluorescence was used for distance measurement. To quantify basal body migration at E16.5, a line was drawn from the center of the hair cell through the basal body to the cell membrane. The distance between the basal body and cell membrane along this line was measured with ImageJ. Hair cells and support cells were readily distinguished by their morphology and position in the epithelium.

Box plots of hair cell measurements were generated using Sigmaplot 11 (Systat Software). The boundary of the box closest to zero indicates the 25th percentile, a line within the box marks the median, and the boundary of the box farthest from zero indicates the 75th percentile. Whiskers (error bars) above and below the box indicate the 90th and 10th percentiles, respectively. Experimental data sets were tested for significance using a Student's t-test in the R software package, and data are presented in the form of mean ± standard error of the mean (s.e.m.).

Organotypic cochlear explant cultures

Explant cultures of the *Kif3a*^{cKO} and littermate control cochleae were established on E18.5, maintained for 3.5 to 4 days in vitro, and processed for each assay. For FM1-43 uptake assays, explants were treated with 5 μM FM1-43 (Invitrogen) for 10 seconds and then washed three times with fresh culture media and imaged immediately. For PAK inhibition experiments, explant cultures from *GFP-CETN2* mice were established on E16.5, treated with 10 μM IPA-3 (Calbiochem) or vehicle (DMSO) the following day, and processed for immunohistochemistry after 3 days in vitro. For Rac1 inhibition experiments, explant cultures from *GFP-CETN2* mice were established on E16.5, treated with 100 μM NSC 23766 (Calbiochem) after 3 hours in vitro, and processed for immunohistochemistry after 2 days in vitro. For quantification of centriole position, samples from three independent experiments were scored as described above.

RESULTS

Kif3a deletion causes PCP-like phenotypes in the organ of Corti

To investigate the function of *Kif3a* in inner ear development, we generated *Kif3a* conditional mutants using a floxed allele of *Kif3a* (Marszalek et al., 2000) and a *Foxg1*^{Cre} allele that drives Cre expression in the otic epithelium, including precursor cells of the OC (Hebert and McConnell, 2000). As the conditional *Kif3a* mutants (referred to as *Kif3a*^{cKO}) die shortly after birth, we first examined cochlear development in vivo at late embryonic stages.

Consistent with an essential role for Kif3a in ciliogenesis, primary cilia were absent from all cochlear epithelial cells as early as E14.5 in *Kif3a*^{cKO} mutants (Fig. 1B). The length of the *Kif3a*^{cKO} cochlea was much shorter than wild type (Fig. 1C,D). At E18.5, wild-type cochleae had a length of 5225 μm ± 149 (n=3). By contrast, *Kif3a*^{cKO} cochleae were 2503 μm ± 104 (n=6) in length. Toward the apex of the *Kif3a*^{cKO} cochlea, many supernumerary rows of hair cells were observed (Fig. 1F, bracket). These defects are reminiscent of PCP/tissue polarity mutant phenotypes and suggest that Kif3a regulates the convergent extension-like movements thought to underlie cochlear extension (Rida and Chen, 2009; Yamamoto et al., 2009).

We next examined hair bundle orientation, another event regulated by the PCP/tissue polarity pathway. In the basal and middle turns of the *Kif3a*^{cKO} OC, where patterning of hair cells and support cells appeared normal, hair bundle orientation defects were mild (Fig. 1G,H,K). Of note, compared with the normal V-shaped hair bundles (Fig. 1G), *Kif3a*^{cKO} hair bundles appeared to have a flattened morphology (Fig. 1H). Toward the apex of the *Kif3a*^{cKO} OC, where the hair cell rows were very disorganized, hair cells with misoriented hair bundles were more prevalent (Fig. 1J,K). We also examined the *Kif3a*^{cKO} utricular macula and observed no overt defect in PCP of utricular hair cells (see Fig. S1 in the supplementary material). Taken together, these results suggest that Kif3a regulates aspects of planar polarity in the OC.

To further assess if PCP/tissue polarity signaling was affected in *Kif3a*^{cKO} OC, we asked whether Kif3a regulates the asymmetric localization of the core PCP proteins dishevelled 2 (Dvl2) and frizzled homolog 3 (Fzd3). In E17.5 wild-type OC, Dvl2-EGFP is localized to the lateral side of hair cell membranes (Wang et al., 2005), whereas Fzd3 is enriched on the medial side of plasma membrane in hair cells and support cells (Wang et al., 2006). Using immunostaining, we found that in the wild type, Dvl2 is asymmetrically localized in hair cells and support cells and appeared enriched on the lateral side of hair cell membranes (Fig. 2A,C,E,G). In the basal region of the *Kif3a*^{cKO} OC, Dvl2 localization was largely normal (Fig. 2B,D), as was the asymmetric localization of Fzd3 (see Fig. S2B,D in the supplementary material). Toward the apex of the *Kif3a*^{cKO} OC, where hair cells and support cells form disorganized rows, asymmetric membrane localization of Dvl2 (Fig. 2F,H) and Fzd3 (see Fig. S2F,H in the supplementary material) was also apparent, albeit somewhat disorganized. Of note, the pattern of Deiters' cells was disturbed in *Kif3a*^{cKO} mutants, particularly toward the apex. In the wild type, the apical extension of a single Deiters' cell can be found in between neighboring hair cells. In *Kif3a*^{cKO} mutants, however, the number and position of Deiters' cell extensions in contact with hair

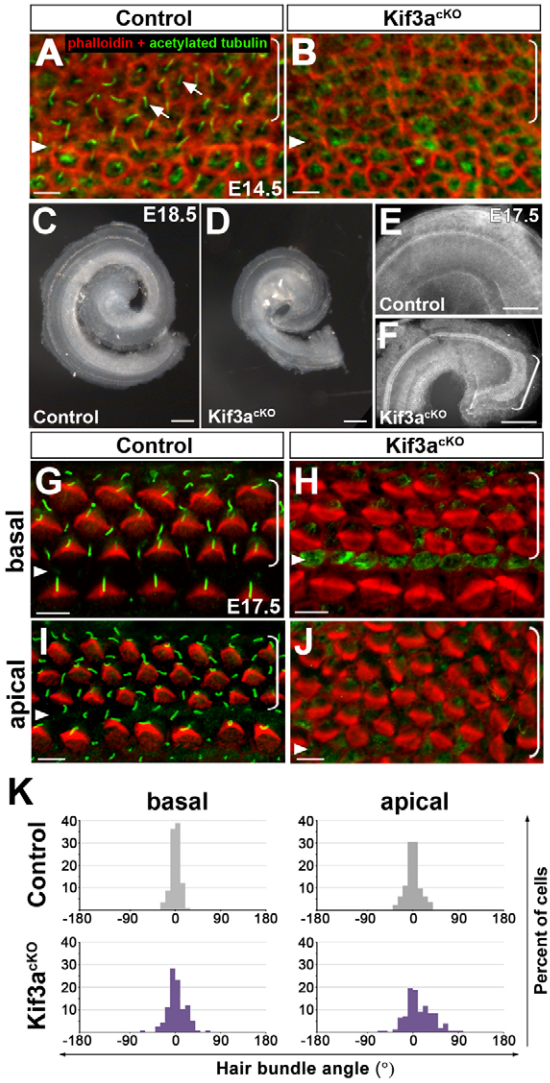

Fig. 1. Cochlear extension and hair bundle orientation defects in Kif3a^{cKO} OC. (**A**,**B**) Acetylated tubulin (green) and phalloidin (red) stained images of E14.5 control (A) and Kif3a^{cKO} (B) OC. Kinocilia are present in control (arrows, A) but undetectable in Kif3a^{cKO} hair cells (B). (**C**,**D**) E18.5 Kif3a^{cKO} cochleae (D) are shorter than controls (C). (**E**,**F**) Kif3a^{cKO} cochleae (stained with phalloidin) exhibit an expansion of hair cell rows near the apex of the cochlea (bracket in F). (**G-J**) Acetylated tubulin (green) and phalloidin (red) staining of control (G,I) and Kif3a^{cKO} (H,J) cochleae at E17.5. Triangles mark the row of pillar cells, and brackets indicate outer hair cell rows. (**K**) Quantification of hair bundle orientation in E18.5 control (basal, n=116; apical, n=82) and Kif3a^{cKO} (basal, n=116; apical, n=154) cochleae. Data are percentages. Scale bars: 5 μm in A,B; 200 μm in C,D; 100 μm in E,F; 5 μm in G-J.

DEVELOPMENT

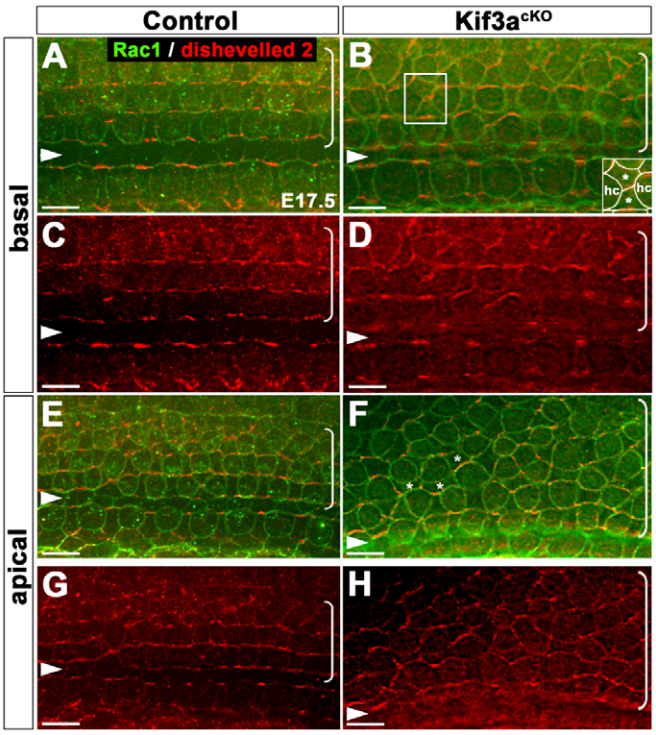

Fig. 2. Localization of dishevelled 2 in Kif3a^{cKO} OC. (**A-H**) Dishevelled 2 immunostaining (red) in basal (A-D) or apical (E-H) regions of E17.5 control and Kif3a^{cKO} OC. Cell boundaries are labeled by Rac1 immunostaining (green). The box in B indicates the apical membranes of two Deiters' cells found in between hair cells and is shown in a schematic diagram in the inset. The asterisks in F indicate examples of abnormal Deiters' cell extensions in contact with hair cells. Triangles indicate the row of pillar cells, and brackets indicate outer hair cell rows. Scale bars: 6 μm. *, support cell; hc, hair cell.

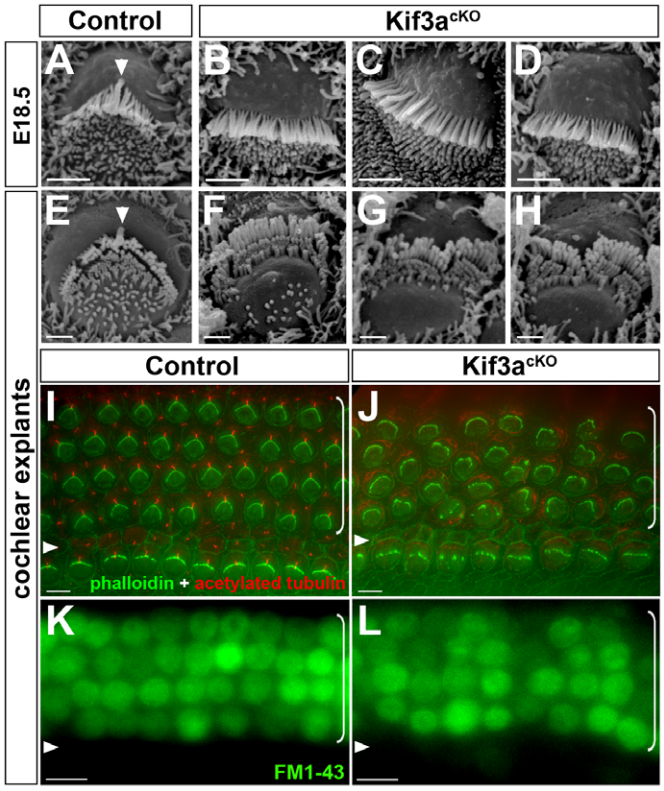

Fig. 3. Kif3a is required for normal hair bundle morphology. (**A-D**) SEMs of control (A) and Kif3a^{cKO} outer hair cells (B-D) from the mid-basal region of E18.5 cochleae. (**E-L**) Hair cell maturation in explant cultures derived from E18.5 cochleae and maintained for 3.5-4 days in vitro. (E-H) SEMs of outer hair cells from control (E) and Kif3a^{cKO} explants (F-H). White triangles in A and E indicate the kinocilium in control cells. (I,J) Control (I) and Kif3a^{cKO} (J) explants stained for acetylated tubulin (red) and phalloidin (green). (K,L) FM1-43 dye (green) uptake is normal in Kif3a^{cKO} explants (L) compared with the control (K). Triangles mark the row of pillar cells, and brackets indicate outer hair cell rows. Scale bars: 1 μm in A-H; 5 μm in I,J; 10 μm in K,L.

cells were abnormal (Fig. 2B,F). Together, these results suggest that PCP/tissue polarity signaling is still active in the *Kif3a^{cKO}* OC, and that Kif3a may regulate support cell movements during cochlear extension.

Kif3a is required for the V shape of the nascent hair bundle

Confirming the light microscopy results (Fig. 1H), SEM analysis showed that *Kif3a^{cKO}* hair cells displayed abnormal hair bundle morphology. At E18.5, in contrast to the normal V shape (Fig. 3A), stereocilia in *Kif3a^{cKO}* hair cells were arranged in straight rows (Fig. 3B-D), indicating that Kif3a is required for the normal V shape of the nascent hair bundle.

To evaluate functional maturation of auditory hair bundles that normally takes place in the early postnatal period (Lelli et al., 2009), we examined hair bundle morphology and FM1-43 dye uptake in explant cultures derived from *Kif3a^{cKO}* cochleae. FM1-43 is a fluorescent styryl dye that can be taken up by hair cells through their mechanotransduction channels upon brief exposure (Gale et al., 2001; Geleoc and Holt, 2003; Meyers et al., 2003). We found that many *Kif3a^{cKO}* hair bundles became fragmented (Fig. 3G,H,J), suggesting that Kif3a is required for hair bundle cohesion. Despite hair bundle deformation, the stereocilia still formed a staircase with graded heights (Fig. 3F-H), and FM1-43 uptake was normal in *Kif3a^{cKO}* explants (Fig. 3L), suggesting that *Kif3a* is dispensable for staircase formation and acquisition of the mechanotransduction apparatus. Of note, many flattened *Kif3a^{cKO}* hair bundles adopted a C shape over time in explant cultures (Fig. 3F,J), probably as a result of remodeling of the cortical actomyosin network in OHCs during the early postnatal period (Etournay et al., 2010).

Kif3a is required for coupling of hair bundle orientation to basal body position

To investigate how Kif3a functions to shape the nascent hair bundle, we examined basal body migration, a key event during hair cell polarization, in *Kif3a^{cKO}* hair cells. To identify the centrioles, we used a GFP-centrin2 transgenic mouse line, which ubiquitously expresses GFP-tagged centrin2, a centrosomal protein (Higginbotham et al., 2004). In the OC, the expression pattern of GFP-centrin2 was identical to that of the centrosomal proteins γ-tubulin and pericentrin (Fig. 4A and data not shown), indicating that it faithfully marks the centrioles. To distinguish between the basal body and the daughter centriole, we made use of an antibody against phospho-β-catenin, which labels the basal body as well as the tips of the stereocilia (Fig. 4A and data not shown). In E18.5

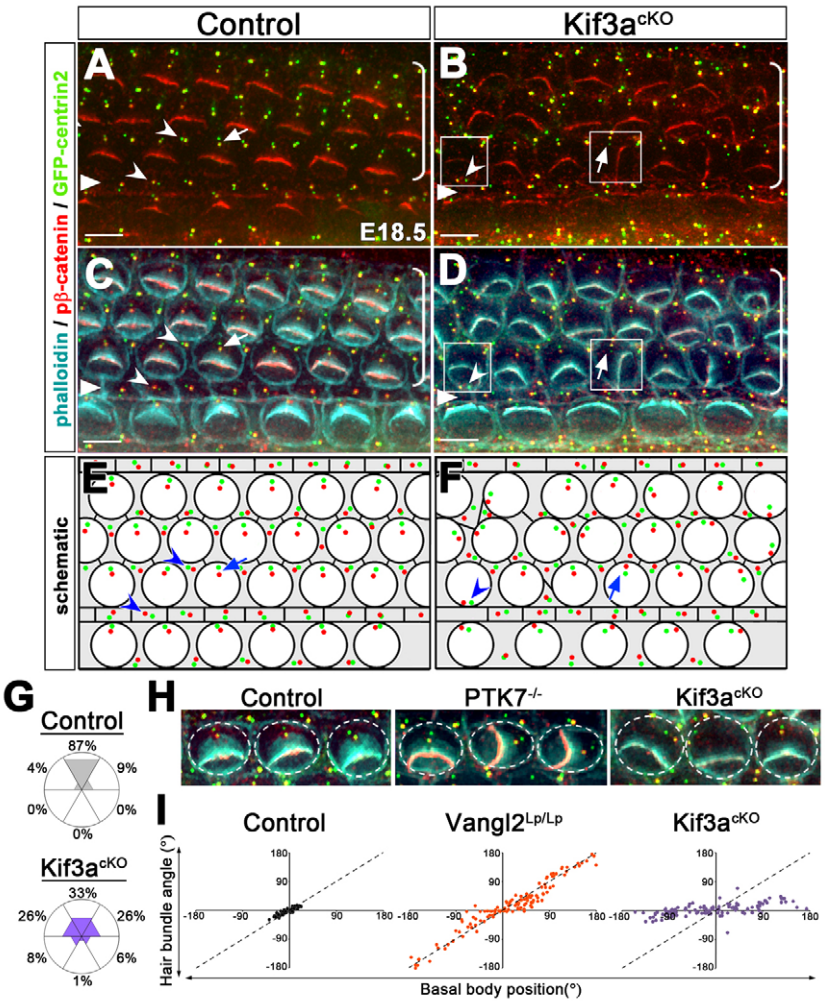

Fig. 4. Uncoupling of hair bundle orientation from basal body position in Kif3a^{cKO} hair cells. (**A-D**) Planar position of centrioles in E18.5 control (A,C) and Kif3a^{cKO} (B,D) hair cells. Green, GFP-centrin2; red, phospho-β-catenin; cyan, phalloidin. Examples of Kif3a^{cKO} hair cells showing uncoupling of hair bundle orientation from basal body position are boxed. Triangles mark the row of pillar cells, and brackets indicate outer hair cell rows. Scale bars: 6 μm. (**E**,**F**) Schematic diagrams of C and D, respectively. Green dots, daughter centrioles; red dots, basal bodies. Support cells are shaded. (**G**) Rose diagrams showing the percentage of centrioles located within the indicated 60° sectors in E18.5 control (shaded gray; *n*=153) and Kif3a^{cKO} (shaded blue; *n*=142) hair cells. (**H**) Hair bundle orientation is coupled with basal body position in wild-type (left) and PTK7$^{-/-}$ (middle) but not Kif3a^{cKO} (right) hair cells. Green, GFP-centrin2; red, phospho-β-catenin; cyan, phalloidin. Hair cell boundaries are outlined by dashed circles. The lateral side of the cochlea is up in all diagrams. (**I**) Scatter plots showing hair bundle orientation in relation to the planar position of the basal body. Control (*n*=73), Vangl2$^{Lp/Lp}$ (*n*=128) and Kif3a^{cKO} (*n*=115) hair cells were all from the mid-basal region of the cochlea. The dashed reference line in each graph indicates a perfect correlation.

wild-type OC, hair cell centrioles were invariably found near the lateral edge of the hair cell, and they displayed remarkable planar polarity: they were aligned along the mediolateral axis with the basal body always positioned medial to the daughter centriole (Fig. 4A,C,E, arrow). Notably, centrioles in the surrounding support cells lacked apparent planar polarity (Fig. 4A,C,E, arrowheads). In E18.5 *Kif3a^{cKO}* hair cells, centrioles have migrated to the edge of hair cells; however, their position along the mediolateral planar polarity axis was severely disrupted (Fig. 4B,D,F). Although most of the centrioles were located in the lateralmost sector in wild-type hair cells, centrioles in *Kif3a^{cKO}* mutants were found at positions all around the edge of the hair cell (Fig. 4G), even near the medial edge (Fig. 4B,D,F, arrowhead).

The severe defect in planar position of basal bodies stood in contrast with the mild hair bundle orientation defects in *Kif3a^{cKO}* hair cells. This prompted us to examine if the coupling between hair bundle orientation and basal body position was affected. In the wild type, there was a tight correlation between bundle orientation and basal body position (Fig. 4H,I; Pearson's coefficient, r=0.9), indicating that hair bundle orientation is coupled with basal body position. This coupling was intact in the PCP mutants examined, including PTK7 (Lu et al., 2004) (Fig. 4H) and *Vangl2$^{Lp/Lp}$*, which is mutant for the core PCP gene Van Gogh-like 2 (Vangl2) (Fig. 4I; r=0.96). In *Kif3a^{cKO}* hair cells, on the other hand, this correlation was lost (Fig. 4H,I; r=0.6). Hair cells with a mispositioned basal body can have normal hair bundle orientation (Fig. 4B,D,F, arrowhead). Conversely, the occasional hair cells with misoriented bundles can have a normally positioned basal body (Fig. 4B,D,F, arrow). These observations demonstrate that in the *Kif3a^{cKO}* mutant, hair bundle orientation is uncoupled from basal body position, and that hair bundle orientation can proceed normally when uncoupled from basal body position.

Kif3a is required for apicobasal positioning of the basal body in hair cells

To further investigate the cause for the uncoupling of hair bundle orientation from basal body position in *Kif3a^{cKO}* mutants, we closely followed the positions of hair cell centrioles over the course of hair bundle development. At E16.5, basal body migration toward the hair cell periphery had occurred in both control and *Kif3a^{cKO}* mutants (Fig. 5A,B). The distance from the basal body to the cell membrane was 1.35 μm + 0.11 in control versus 1.21 μm + 0.09 in *Kif3a^{cKO}* hair cells (P=0.34), confirming that Kif3a is not required for basal body migration. However, there was a striking difference in basal body position along the apicobasal axis between control and *Kif3a^{cKO}* hair cells. The basal body in wild-type hair cells was positioned just underneath the apical surface, and the daughter centriole was positioned more basally (Fig. 5C). By contrast, in *Kif3a^{cKO}* hair cells, the basal body appeared to have descended to the same level as the daughter centriole (Fig. 5D). The aberrant positioning of the basal body persisted through later developmental stages (E17.5 and E18.5) in *Kif3a^{cKO}* hair cells (Fig. 5F,K). By

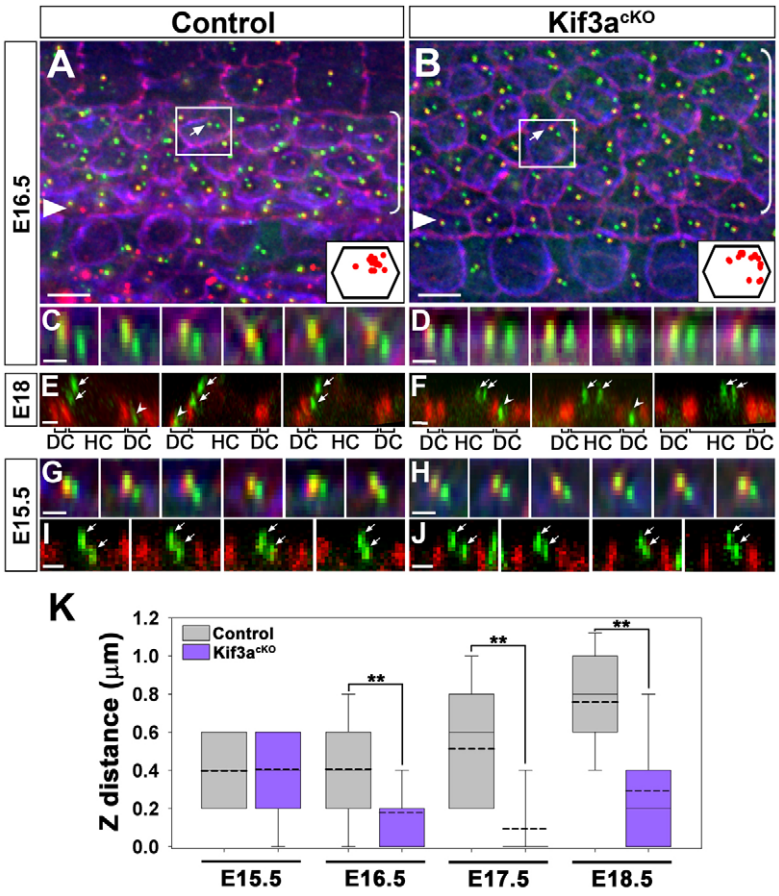

Fig. 5. Aberrant apicobasal positioning of basal body in Kif3a^{cKO} hair cells. (**A**,**B**) Basal body migration in E16.5 control (A) and Kif3a^{cKO} (B) hair cells. Green, GFP-centrin2; red, phospho-β-catenin; blue, phalloidin. Schematic diagrams summarizing the planar positions of the hair cell basal bodies are shown in the insets. Triangles mark the row of pillar cells, and brackets indicate outer hair cell rows. (**C**,**D**) Optical slices along the *z*-axis of E16.5 control (C) or Kif3a^{cKO} (D) hair cells showing the apicobasal position of the centriole pairs. (**E**,**F**) Optical slices along the *z*-axis showing the apicobasal position of hair cell centrioles relative to the tight junctions (as marked by ZO-1 immunostaining) in E18.5 control (E) and Kif3a^{cKO} (F) OC. Green, GFP-centrin2; red, ZO-1. Brackets indicate the domains of hair cells (HC) and Deiters' cells (DC) demarcated by ZO-1 staining. Arrows indicate hair cell centrioles. Arrowheads indicate the centrioles of DC. (**G-J**) Optical slices along the *z*-axis showing normal apicobasal position of centrioles in Kif3a^{cKO} hair cells (H,J) compared with controls (G,I) at E15.5. (G,H) Green, GFP-centrin2; red, phospho-β-catenin; blue, phalloidin. (I,J) Green, GFP-centrin2; red, ZO-1. (**K**) Distance along the *z*-axis between the basal body and the daughter centriole in control (shaded gray) and Kif3a^{cKO} (shaded blue) hair cells at different developmental stages. Compared with controls, the *z* distance between centriole pairs in Kif3a^{cKO} mutant hair cells is similar at E15.5, but significantly shorter at E16.5, E17.5 and E18.5. $^{**}P<0.001$. Broken lines indicate the mean. Scale bars: 5 μm in A,B; 1 μm in C-J.

contrast, basal body positioning in *Kif3a^{cKO}* support cells (pillar and Deiters' cells) was not affected compared with controls (data not shown). These results indicate that Kif3a regulates basal body positioning along the apicobasal axis of hair cells.

The apicobasal positioning defect of the basal body in *Kif3a^{cKO}* hair cells may reflect a requirement of Kif3a in apical docking of the basal body at the onset of ciliogenesis. We therefore examined basal body positioning at E15.5, before basal body migration. We found that the apicobasal position of the basal body was normal in *Kif3a^{cKO}* hair cells compared with controls (Fig. 5G-K). Therefore, we conclude that Kif3a is not required for the initial apical docking of the basal body. Taken together, our results reveal that Kif3a controls an active developmental process that positions the basal body along both the apicobasal and planar polarity axes during hair cell polarization and raise the possibility that uncoupling of hair bundle orientation from basal body position may be related to the aberrant basal body position in *Kif3a^{cKO}* mutants.

Kif3a regulates cortical PAK activity during hair cell polarization

To investigate the mechanisms by which Kif3a regulates basal body positioning in hair cells, we hypothesized that Kif3a is involved in generating or transducing a hair cell-intrinsic polarity cue to position the basal body near the lateral membrane. Previously, we discovered that activated PAKs, cytoskeletal regulators downstream of the small GTPases Rac and Cdc42 (Bokoch, 2003), are asymmetrically distributed in developing auditory hair cells, as detected by an antibody specific for phosphorylated PAK (pPAK) (Grimsley-Myers et al., 2009). Both the developmental onset of PAK activation and its subcellular localization coincide with migration of the basal body to the lateral edge of hair cells, making PAK an attractive candidate component of the hair cell polarity machinery. During normal development, cortical localization of pPAK was first detected in hair cells between E16.5 and E17.5 at the base of the cochlea, where the basal body has migrated to the periphery (Grimsley-Myers et al., 2009). By E17.5, pronounced pPAK staining correlated with the locations of hair cell centrioles (Fig. 6A,B,E). Just beneath the apical cell surface, pPAK was localized in a triangle-shaped ring around the basal body and the stereocilia insertion sites. We found that the basal body was stereotypically positioned at the lateral tip of the ring (Fig. 6A,G). Around 1 μm basal to the ring, pPAK was asymmetrically localized to the lateral side of the hair cell membrane, immediately adjacent to the location of the daughter centriole (Fig. 6B,G′).

In the *Kif3a^{cKO}* mutant, pPAK staining was present but disorganized at both subcellular locations (Fig. 6C,D,F). At the base of the hair bundle, pPAK staining lost its triangular pattern and instead conformed to the shape of the flat bundle (Fig. 6C,H,I,J). Strikingly, basal bodies were no longer positioned within the ring of pPAK staining around the base of the hair bundle. Instead, both centrioles were located approximately 1 μm below the base of the hair bundle, closely juxtaposed with the plasma membrane (arrows, Fig. 6D; Fig. 6D,H′,I′,J′). At this level, instead of the normal horseshoe-shaped pattern on the lateral membrane, pPAK was localized around the entire perimeter of the plasma membrane, albeit still relatively enriched on the lateral side (Fig. 6D,H′,I′,J′). These results suggest that Kif3a regulates localized PAK activation at the hair cell cortex adjacent to the centrioles, and show an intriguing correlation between mislocalized PAK activity and basal body positioning defects in *Kif3a^{cKO}* hair cells.

DEVELOPMENT

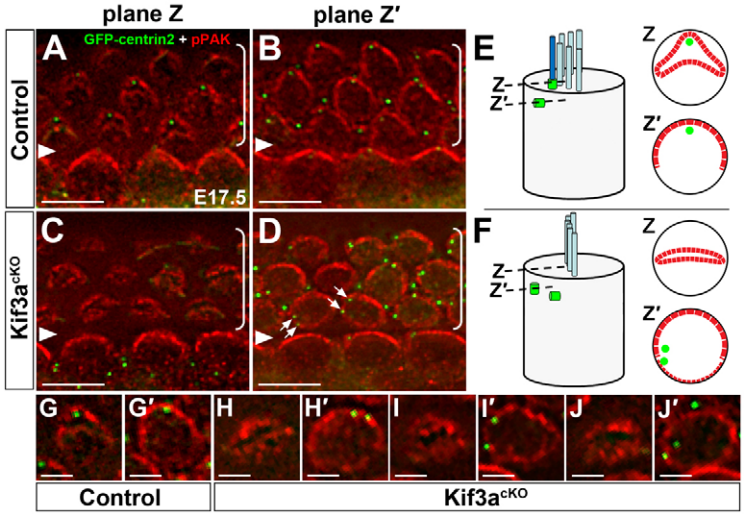

Fig. 6. Abnormal phospho-PAK localization correlates with centriole defects in Kif3a^{cKO} hair cells. (**A-D**) Single *z*-sections showing centriole (green, GFP-centrin2) location in relation to phospho-PAK staining (red) in E17.5 control (A,B) and Kif3a^{cKO} (C,D) hair cells. Plane Z′ is approximately 1 μm basal to plane Z. Arrows in D indicate aberrantly positioned centriole pairs. Triangles mark the row of pillar cells, and brackets indicate outer hair cell rows. (**E**,**F**) Schematic diagrams of centriole positions relative to pPAK localization in a control (E) and a Kif3a^{cKO} (F) hair cell. On the left are side views of a hair cell showing centriole (green barrels) positions relative to the hair bundle. Circles to the right represent cross sections through the hair cell at plane Z and plane Z′ and show the localization of pPAK (red) and the position of the centrioles (green dots). (**G-J′**) Higher magnification images of single *z*-sections showing pPAK localization (red) and centriole (green, GFP-centrin2) location at plane Z (G,H,I,J) and Z′ (G′,H′,I′,J′) in control (G,G′) and Kif3a^{cKO} hair cells (H-J′). Scale bars: 6 μm in A-D; 3 μm in G-J′.

Rac-PAK signaling regulates basal body positioning and hair bundle morphogenesis

If PAK activity is indeed a polarity cue that mediates basal body positioning downstream of Kif3a, then PAK signaling should be required for correct basal body positioning in hair cells. To test this hypothesis, we applied IPA-3, a small-molecule inhibitor of PAK (Deacon et al., 2008), to cochlear explants and assessed the effect on basal body positioning and hair bundle morphogenesis. We found that IPA-3 treatment resulted in basal body positioning defects, as well as bundle morphology and orientation defects (Fig. 7B,C). Because PAK kinases are downstream effectors of the small GTPases Rac and Cdc42, we also tested if Rac activity is required for basal body positioning by treating cochlear explants with NSC 23766, a small molecule inhibitor of Rac (Gao et al., 2004). We found that Rac inhibition also resulted in basal body positioning and bundle morphogenesis defects (Fig. 7E,F). Of note, kinocilia were present in inhibitor-treated explants (see Fig. S3 in the supplementary material), suggesting that the basal body positioning defect is due to impaired Rac-PAK signaling rather than the absence of the kinocilium. Taken together, these results support the hypothesis that Rac-PAK signaling acts downstream of Kif3a to regulate basal body positioning during hair cell polarization.

DISCUSSION

In this study, we identify the kinesin-II subunit Kif3a as a key component of the hair cell-intrinsic polarity machinery that couples hair bundle morphogenesis and orientation with basal body positioning. In *Kif3a^{cKO}* hair cells, in addition to the absence of the kinocilium, basal body positioning along both epithelial polarity axes was disrupted, hair bundles failed to develop the stereotypical V shape, and their orientation became uncoupled from basal body position. These phenotypes indicate that, by serving the dual functions of IFT and intracellular transport, Kif3a coordinates planar polarization of the hair bundle and the centrioles.

Both *Kif3a^{cKO}* and *Ift88* mutants (Jones et al., 2008) lack primary cilia and display PCP/tissue polarity defects, including shortened cochlear ducts and hair bundle misorientation, demonstrating a general requirement of the primary cilium/basal body for tissue polarity. Interestingly, while the PCP/tissue polarity pathway acts in both hearing and vestibular organs, neither *Kif3a* nor *Ift88* (Jones et al., 2008) mutations appear to affect PCP of utricular hair cells. It is conceivable that cell-cell interactions necessary for the propagation of polarity signals are different in hearing and balance organs owing to their distinct mosaic patterns of hair cells and support cells. Moreover, distinct expression patterns of cell-adhesion molecules may contribute to differences in cell-adhesion and cytoskeletal organization between hearing and balance organs (Hackett et al., 2002; Simonneau et al., 2003). Interestingly, there is evidence that an additional, as yet unidentified, patterning event operates together with the tissue polarity pathway to regulate PCP in the utricular macula (Deans et al., 2007).

The signaling events mediated by the IFT molecules during cochlear extension remain to be elucidated. An intriguing possible role of cilia/IFT is to maintain the balance between Wnt/β-catenin and Wnt/PCP signaling; however, experimental evidence for this idea is controversial (Corbit et al., 2008; Gerdes et al., 2007; Huang and Schier, 2009; Ocbina et al., 2009). We did not detect changes in the localization of β-catenin or phospho-β-catenin in *Kif3a^{cKO}* OC, although it is possible that there are quantitative differences not revealed by immunofluorescence. β-catenin was localized to cellular junctions (data not shown), whereas phospho-β-catenin, destined for proteosome-mediated degradation, was localized to cellular junctions, the basal body and the tips of the stereocilia. Others have reported localization of phospho-β-catenin to the centrosome of cultured cells (Corbit et al., 2008; Huang et al., 2007). The significance of the different localization of β-catenin versus phospho-β-catenin that we observed in hair cells is currently unknown.

Furthermore, using a transgenic Wnt-signaling reporter line, BATgal, which expresses *LacZ* under the control of *Tcf/Lef* binding sites (Maretto et al., 2003), we did not observe any overt changes in the level of Wnt/β-catenin signaling in *Kif3a^{cKO}* cochleae by X-gal staining (data not shown). *Kif3a* deletion in mouse embryonic fibroblasts causes hyperphosphorylation of Dishevelled proteins (Corbit et al., 2008). We showed that Kif3a is not required for asymmetric localization of Dvl2 in the OC, but it remains possible that Kif3a may regulate the activity of Dishevelled proteins in the OC. At present the relative contributions by hair cells and support cells to cochlear extension is not known. In the *Kif3a^{cKO}* OC, we often observed multiple Deiters' cells in contact with one hair cell, particularly in the apical region, where the hair cell rows were very disorganized. This suggests that Deiters' cell movements could be regulated by Kif3a and may play a role in cochlear extension.

Our cochlear explant experiments further delineate the role of Kif3a in hair bundle morphogenesis. Kif3a function is important for the V shape of the nascent hair bundle, and for the structural cohesion of the hair bundle during functional maturation. However,

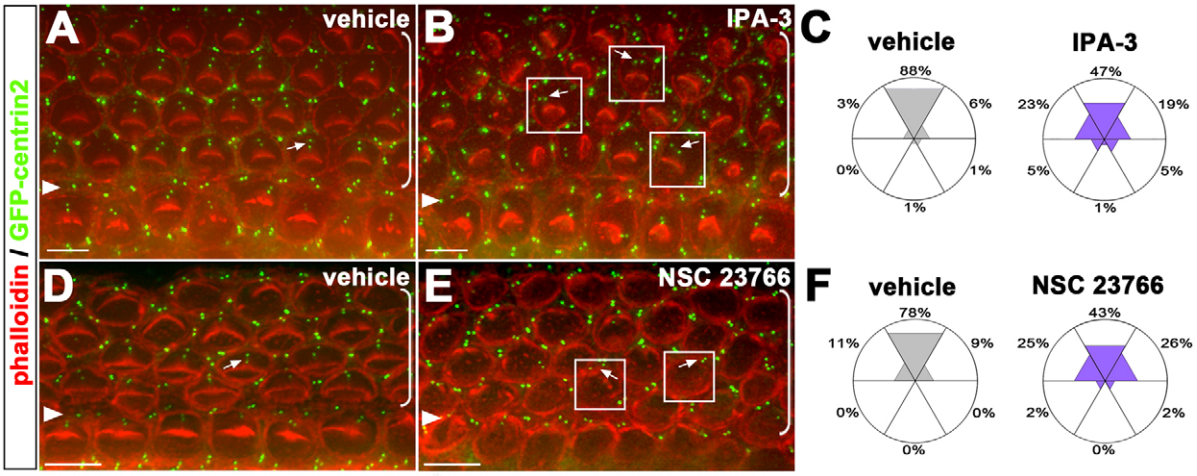

Fig. 7. Rac-PAK signaling regulates hair cell-centriole positioning. (**A**,**B**) Cochlear explants treated with vehicle (A) or 10 μM IPA-3 (B). Green, GFP-centrin2; red, phalloidin staining. Arrows indicate centriole pairs. Examples of hair cells with centriole-positioning defects are boxed in B. Triangles mark the row of pillar cells, and brackets indicate outer hair cell rows. (**C**) Rose diagrams showing the percentage of centrioles located within the indicated 60° sectors in hair cells of explants treated with vehicle (shaded gray, *n*=270) or 10 μM IPA-3 (shaded blue, *n*=432). (**D**,**E**) Cochlear explants treated with vehicle (D) or 100 μM NSC 23766 (E). Arrows indicate centriole pairs. Examples of hair cells with mispositioned centrioles are boxed in E. (**F**) Rose diagrams showing the percentage of centrioles located within the indicated 60° sectors in hair cells of explants treated with vehicle (shaded gray, *n*=218) or 100 μM NSC 23766 (shaded blue, *n*=218). The lateral side of the cochlea is up in all diagrams. Scale bars: 5 μm in A,B; 5 μm in D,E.

Kif3a and the kinocilium are dispensible for selective elongation of the stereocilia (staircase formation) or acquisition of the mechanotransduction apparatus. Consistent with our results, in PCDH15-ΔCD2 mutant hair cells, where the kinocilium became detached from the hair bundle, staircase formation and mechanotransduction were also unaffected (Webb et al., 2011).

Although both *Kif3a*^{cKO} and *Ift88* (Jones et al., 2008) mutants have defects in bundle orientation and planar positioning of the basal body, there are important differences in their phenotypes. By comparing the differences, we can begin to tease apart the ciliary and non-ciliary functions of Kif3a in hair cell development. In contrast to *Ift88* mutants, in which a fraction of hair cells form circular hair bundles with a centrally positioned basal body (Jones et al., 2008), we did not observe any circular hair bundle or centrally positioned basal body in *Kif3a*^{cKO} mutants, indicating that Kif3a is not required for basal body migration. Another key difference in the phenotypes lies in the coupling between basal body position and hair bundle orientation. In *Ift88* mutants, hair bundle orientation defects strongly correlated with basal body positioning defects (Jones et al., 2008). By contrast, we show that in *Kif3a*^{cKO} hair cells, hair bundle orientation is no longer coupled with basal body position, and basal bodies are mispositioned along both apicobasal and planar polarity axes. These phenotypes are novel and striking in that they are not observed in previously reported PCP or ciliogenesis (*Ift88*) mutants. These results suggest that coupling of hair bundle orientation and basal body position is, at least in part, mediated by a non-ciliary function of Kif3a. Interestingly, it has been suggested recently that the links between the kinocilium and stereocilia also play a role in coordinating hair bundle orientation and basal body position (Webb et al., 2011).

We present evidence for a non-ciliary function of Kif3a in regulating cortical PAK activity. PAK activity exhibits several key properties of a polarity cue. First, it is asymmetrically localized in hair cells. Second, it is required for normal basal body positioning. Third, in *Kif3a*^{cKO} hair cells, mislocalized PAK activity correlated with basal body positioning defects, suggesting that the precise spatial pattern of PAK activation might also be important. Together with our previous findings, these results reveal multiple crucial functions of PAK signaling in hair bundle morphogenesis. During the early phase of hair bundle formation, cortical PAK activity serves to position the basal body and direct hair bundle orientation. Subsequently, PAK signaling is required for the cohesion of the nascent hair bundles (Grimsley-Myers et al., 2009). As a motor molecule, Kif3a may regulate PAK activity through direct or indirect mechanisms. As our in vitro results indicate that both Rac and PAK signaling are required for basal body positioning, we speculate that Kif3a may transport a cargo that in turn regulates activation of Rac GTPases at cortical locations. Alternatively, Kif3a may transport a cargo that mediates the interaction between microtubules and cortical actin, thereby regulating cortical PAK activity.

Taken together, our results support the argument that the hair cell intrinsic polarity machinery regulated by Kif3a acts in parallel to the PCP/tissue polarity pathway. First, we showed previously that the formation of the asymmetric pPAK domain per se was not affected in *Vangl2*$^{Lp/Lp}$ mutants; rather, it is misoriented in a manner that precisely correlates with hair bundle misorientation (Grimsley-Myers et al., 2009). Thus, in PCP mutants, individual hair cells were able to polarize in response to hair cell-intrinsic cues, using both morphological (V-shaped hair bundle) and molecular criteria (asymmetric pPAK localization). By contrast, both forms of readout for hair cell polarization were disrupted in *Kif3a*^{cKO} mutants: hair bundles adopted a flattened morphology and pPAK staining became mislocalized around hair cell membranes. Second, Kif3a, but neither PTK7 nor Vangl2 (data not shown), is required for correct apicobasal positioning of the basal body. Third, there is evidence that PCP signaling is still active in *Kif3a*^{cKO} mutants. The core PCP proteins Dvl2 and Fzd3 were still asymmetrically localized in the *Kif3a*^{cKO} OC. Moreover, cortical PAK activity, though diffused around the hair cell membrane, was still somewhat enriched on the lateral side, suggesting that PAK activity is still regulated by tissue polarity cues

in *Kif3a*^{cKO} mutants. Finally, hair bundle misorientation in *Kif3a*^{cKO} mutants was mild compared with the PCP mutants. Together, our data provide strong support for the model that the Kif3a-mediated cell-intrinsic pathway and the PCP/tissue polarity pathway act in concert and converge on PAK kinases to regulate hair cell polarity.

Acknowledgements
We thank Paul Adler, Gwenaëlle Géléoc, Kevin Pfister, Jing Yu and members of the Lu laboratory for helpful comments on the manuscript; Larry Goldstein and Matthias Hebrok for mice; Jeremy Nathans, Yanshu Wang, Jeffrey Salisbury, Bradley Yoder and Xiaowu Zhang for antibodies. This study was supported by the NIH grant RO1 DC009238 (to X.L.). C.W.S. was supported by NIH training grant T32 GM008136 for Cell and Molecular Biology at the University of Virginia. Deposited in PMC for release after 12 months.

Competing interests statement
The authors declare no competing financial interests.

Supplementary material
Supplementary material for this article is available at
http://dev.biologists.org/lookup/suppl/doi:10.1242/dev.065961/-/DC1

References
Bokoch, G. M. (2003). Biology of the p21-activated kinases. *Annu. Rev. Biochem.* **72**, 743-781.
Corbit, K. C., Shyer, A. E., Dowdle, W. E., Gaulden, J., Singla, V., Chen, M. H., Chuang, P. T. and Reiter, J. F. (2008). Kif3a constrains beta-catenin-dependent Wnt signalling through dual ciliary and non-ciliary mechanisms. *Nat. Cell Biol.* **10**, 70-76.
Deacon, S. W., Beeser, A., Fukui, J. A., Rennefahrt, U. E., Myers, C., Chernoff, J. and Peterson, J. R. (2008). An isoform-selective, small-molecule inhibitor targets the autoregulatory mechanism of p21-activated kinase. *Chem. Biol.* **15**, 322-331.
Deans, M. R., Antic, D., Suyama, K., Scott, M. P., Axelrod, J. D. and Goodrich, L. V. (2007). Asymmetric distribution of prickle-like 2 reveals an early underlying polarization of vestibular sensory epithelia in the inner ear. *J. Neurosci.* **27**, 3139-3147.
Etournay, R., Lepelletier, L., Boutet de Monvel, J., Michel, V., Cayet, N., Leibovici, M., Weil, D., Foucher, I., Hardelin, J. P. and Petit, C. (2010). Cochlear outer hair cells undergo an apical circumference remodeling constrained by the hair bundle shape. *Development* **137**, 1373-1383.
Gale, J. E., Marcotti, W., Kennedy, H. J., Kros, C. J. and Richardson, G. P. (2001). FM1-43 dye behaves as a permeant blocker of the hair-cell mechanotransducer channel. *J. Neurosci.* **21**, 7013-7025.
Gao, Y., Dickerson, J. B., Guo, F., Zheng, J. and Zheng, Y. (2004). Rational design and characterization of a Rac GTPase-specific small molecule inhibitor. *Proc. Natl. Acad. Sci. USA* **101**, 7618-7623.
Geleoc, G. S. and Holt, J. R. (2003). Developmental acquisition of sensory transduction in hair cells of the mouse inner ear. *Nat. Neurosci.* **6**, 1019-1020.
Gerdes, J. M., Liu, Y., Zaghloul, N. A., Leitch, C. C., Lawson, S. S., Kato, M., Beachy, P. A., Beales, P. L., DeMartino, G. N., Fisher, S. et al. (2007). Disruption of the basal body compromises proteasomal function and perturbs intracellular Wnt response. *Nat. Genet.* **39**, 1350-1360.
Gillespie, P. G. and Muller, U. (2009). Mechanotransduction by hair cells: models, molecules, and mechanisms. *Cell* **139**, 33-44.
Goetz, S. C. and Anderson, K. V. (2010). The primary cilium: a signalling centre during vertebrate development. *Nat. Rev. Genet.* **11**, 331-344.
Grimsley-Myers, C. M., Sipe, C. W., Geleoc, G. S. and Lu, X. (2009). The small GTPase Rac1 regulates auditory hair cell morphogenesis. *J. Neurosci.* **29**, 15859-15869.
Hackett, L., Davies, D., Helyer, R., Kennedy, H., Kros, C., Lawlor, P., Rivolta, M. N. and Holley, M. (2002). E-cadherin and the differentiation of mammalian vestibular hair cells. *Exp. Cell Res.* **278**, 19-30.
Hebert, J. M. and McConnell, S. K. (2000). Targeting of cre to the Foxg1 (BF-1) locus mediates loxP recombination in the telencephalon and other developing head structures. *Dev. Biol.* **222**, 296-306.
Higginbotham, H., Bielas, S., Tanaka, T. and Gleeson, J. G. (2004). Transgenic mouse line with green-fluorescent protein-labeled Centrin 2 allows visualization of the centrosome in living cells. *Transgenic Res.* **13**, 155-164.
Huang, P. and Schier, A. F. (2009). Dampened Hedgehog signaling but normal Wnt signaling in zebrafish without cilia. *Development* **136**, 3089-3098.
Huang, P., Senga, T. and Hamaguchi, M. (2007). A novel role of phospho-beta-catenin in microtubule regrowth at centrosome. *Oncogene* **26**, 4357-4371.
Jagger, D., Collin, G., Kelly, J., Towers, E., Nevill, G., Longo-Guess, C., Benson, J., Halsey, K., Dolan, D., Marshall, J. et al. (2011). Alstrom Syndrome protein ALMS1 localizes to basal bodies of cochlear hair cells and regulates cilium-dependent planar cell polarity. *Hum. Mol. Genet.* **20**, 466-481.
Jones, C., Roper, V. C., Foucher, I., Qian, D., Banizs, B., Petit, C., Yoder, B. K. and Chen, P. (2008). Ciliary proteins link basal body polarization to planar cell polarity regulation. *Nat. Genet.* **40**, 69-77.
Lefevre, G., Michel, V., Weil, D., Lepelletier, L., Bizard, E., Wolfrum, U., Hardelin, J. P. and Petit, C. (2008). A core cochlear phenotype in USH1 mouse mutants implicates fibrous links of the hair bundle in its cohesion, orientation and differential growth. *Development* **135**, 1427-1437.
Lelli, A., Asai, Y., Forge, A., Holt, J. R. and Geleoc, G. S. (2009). Tonotopic gradient in the developmental acquisition of sensory transduction in outer hair cells of the mouse cochlea. *J. Neurophysiol.* **101**, 2961-2973.
Lu, X., Borchers, A. G., Jolicoeur, C., Rayburn, H., Baker, J. C. and Tessier-Lavigne, M. (2004). PTK7/CCK-4 is a novel regulator of planar cell polarity in vertebrates. *Nature* **430**, 93-98.
Maretto, S., Cordenonsi, M., Dupont, S., Braghetta, P., Broccoli, V., Hassan, A. B., Volpin, D., Bressan, G. M. and Piccolo, S. (2003). Mapping Wnt/beta-catenin signaling during mouse development and in colorectal tumors. *Proc. Natl. Acad. Sci. USA* **100**, 3299-3304.
Marszalek, J. R., Ruiz-Lozano, P., Roberts, E., Chien, K. R. and Goldstein, L. S. (1999). Situs inversus and embryonic ciliary morphogenesis defects in mouse mutants lacking the KIF3A subunit of kinesin-II. *Proc. Natl. Acad. Sci. USA* **96**, 5043-5048.
Marszalek, J. R., Liu, X., Roberts, E. A., Chui, D., Marth, J. D., Williams, D. S. and Goldstein, L. S. (2000). Genetic evidence for selective transport of opsin and arrestin by kinesin-II in mammalian photoreceptors. *Cell* **102**, 175-187.
May-Simera, H. L., Ross, A., Rix, S., Forge, A., Beales, P. L. and Jagger, D. J. (2009). Patterns of expression of Bardet-Biedl syndrome proteins in the mammalian cochlea suggest noncentrosomal functions. *J. Comp. Neurol.* **514**, 174-188.
Meyers, J. R., MacDonald, R. B., Duggan, A., Lenzi, D., Standaert, D. G., Corwin, J. T. and Corey, D. P. (2003). Lighting up the senses: FM1-43 loading of sensory cells through nonselective ion channels. *J. Neurosci.* **23**, 4054-4065.
Montcouquiol, M., Rachel, R. A., Lanford, P. J., Copeland, N. G., Jenkins, N. A. and Kelley, M. W. (2003). Identification of Vangl2 and Scrb1 as planar polarity genes in mammals. *Nature* **423**, 173-177.
Moser, J. J., Fritzler, M. J., Ou, Y. and Rattner, J. B. (2010). The PCM-basal body/primary cilium coalition. *Semin. Cell Dev. Biol.* **21**, 148-155.
Nigg, E. A. and Raff, J. W. (2009). Centrioles, centrosomes, and cilia in health and disease. *Cell* **139**, 663-678.
Nishimura, T., Kato, K., Yamaguchi, T., Fukata, Y., Ohno, S. and Kaibuchi, K. (2004). Role of the PAR-3-KIF3 complex in the establishment of neuronal polarity. *Nat. Cell Biol.* **6**, 328-334.
Ocbina, P. J., Tuson, M. and Anderson, K. V. (2009). Primary cilia are not required for normal canonical Wnt signaling in the mouse embryo. *PLoS ONE* **4**, e6839.
Rida, P. C. and Chen, P. (2009). Line up and listen: planar cell polarity regulation in the mammalian inner ear. *Semin. Cell Dev. Biol.* **20**, 978-985.
Ross, A. J., May-Simera, H., Eichers, E. R., Kai, M., Hill, J., Jagger, D. J., Leitch, C. C., Chapple, J. P., Munro, P. M., Fisher, S. et al. (2005). Disruption of Bardet-Biedl syndrome ciliary proteins perturbs planar cell polarity in vertebrates. *Nat. Genet.* **37**, 1135-1140.
Simonneau, L., Gallego, M. and Pujol, R. (2003). Comparative expression patterns of T-, N-, E-cadherins, beta-catenin, and polysialic acid neural cell adhesion molecule in rat cochlea during development: implications for the nature of Kolliker's organ. *J. Comp. Neurol.* **459**, 113-126.
Simons, M. and Mlodzik, M. (2008). Planar cell polarity signaling: from fly development to human disease. *Annu. Rev. Genet.* **42**, 517-540.
Takeda, S., Yonekawa, Y., Tanaka, Y., Okada, Y., Nonaka, S. and Hirokawa, N. (1999). Left-right asymmetry and kinesin superfamily protein KIF3A: new insights in determination of laterality and mesoderm induction by kif3A$^{-/-}$ mice analysis. *J. Cell Biol.* **145**, 825-836.
Teng, J., Rai, T., Tanaka, Y., Takei, Y., Nakata, T., Hirasawa, M., Kulkarni, A. B. and Hirokawa, N. (2005). The KIF3 motor transports N-cadherin and organizes the developing neuroepithelium. *Nat. Cell Biol.* **7**, 474-482.
Tilney, L. G., Tilney, M. S. and DeRosier, D. J. (1992). Actin filaments, stereocilia, and hair cells: how cells count and measure. *Annu. Rev. Cell Biol.* **8**, 257-274.
Wang, J., Mark, S., Zhang, X., Qian, D., Yoo, S. J., Radde-Gallwitz, K., Zhang, Y., Lin, X., Collazo, A., Wynshaw-Boris, A. et al. (2005). Regulation of polarized extension and planar cell polarity in the cochlea by the vertebrate PCP pathway. *Nat. Genet.* **37**, 980-985.
Wang, Y., Guo, N. and Nathans, J. (2006). The role of Frizzled3 and Frizzled6 in neural tube closure and in the planar polarity of inner-ear sensory hair cells. *J. Neurosci.* **26**, 2147-2156.
Webb, S. W., Grillet, N., Andrade, L. R., Xiong, W., Swarthout, L., Della Santina, C. C., Kachar, B. and Muller, U. (2011). Regulation of PCDH15 function in mechanosensory hair cells by alternative splicing of the cytoplasmic domain. *Development* **138**, 1607-1617.
Yamamoto, N., Okano, T., Ma, X., Adelstein, R. S. and Kelley, M. W. (2009). Myosin II regulates extension, growth and patterning in the mammalian cochlear duct. *Development* **136**, 1977-1986.